Sparse MIMO linear array imaging based on Localized Low-rank Promoting algorithm

Chen Qiao[1,a], Tong Ningning[1,b], Wei Wei[2,c,] Yan Chong[2,d]

[1]Air Force Engineering University

[2]Air Force Logistics Institute

[a]1498682392@qq.com

[b]1043961004@qq.com

[c]1125084795@qq.com

[d]1137366857@qq.com

Abstract. In order to improve the image quality of (Multiple-Input Multiple-Output, MIMO) sparse linear array, this paper deeply explored the block sparse characteristics of imaging targets. By introducing LLP algorithm, firstly, the elements of echo signal are divided into 4-length blocks, and each block matrix is transformed into 2-2-size matrix. By using a logarithmic determinant function which has the ability to promote the block-sparsity and local smoothness simultaneously, the low rank of these 2 × 2 matrices is improved. Finally, the iterative weighting method can efficiently reconstruct the objective image by iteratively minimizing a surrogate function of the original objective function. Simulation results show that the proposed method can get higher quality target image than the traditional algorithm.

1. Introduction

Through the effective remote sensing technology, it is an important research direction of modern radar technology to obtain the two-dimensional image of airspace target, which is widely used in military and civil fields. As a new radar system, MIMO radar obtains more virtual array than the real array by the characteristics of multi transmit and multi receive array structure, and uses space sampling instead of time sampling to achieve the imaging effect of single snapshot. Wang H studied a single snapshot MIMO imaging algorithm, but the number of array elements is still relatively large and the system is relatively complex[1]. On this basis, Chen G studied sparse array imaging technology to effectively reduce array elements while ensuring the quality of imaging, and studies the problem of data loss[2]. In the face of sparse array imaging, compressed sensing is an effective signal processing and image restoration technology. By solving a sparse constraint problem, sparse signals can be recovered from incomplete observation vectors. In recent years, the imaging algorithm based on compressed sensing has made rapid development [3,4]. The theory of compressed sensing (CS) is applied to MIMO radar, which overcomes the defect of sparse array and realizes single snapshot imaging[5]. However, the traditional sparse recovery algorithm often does not consider the target block aggregation characteristics[6], ignoring the block structure characteristics of the echo signal, and the imaging performance needs to be further improved. Aiming at the problem that the traditional CS algorithm can't take advantage of the block sparseness of MIMO target, this paper adopts a block sparseness

reconstruction LLP (localized low range promoting) algorithm[7] for MIMO sparse linear array imaging. The simulation results show that the proposed algorithm improves the image quality.

2. The imaging signal model of MIMO sparse linear array

On the premise of performance guarantee, sparse MIMO radar array can reduce the number of elements, reduce the hardware complexity and improve the flexibility of system design. A sparse MIMO linear array is presented[5], as shown in Figure 4.1. Compared with the uniform linear array, the transmitting array does not change (it is still a uniform arrangement of transmitting array elements), and the receiving array elements are sparse.

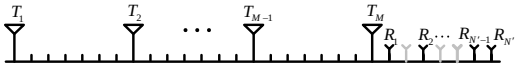

(a) MIMO sparse linear array

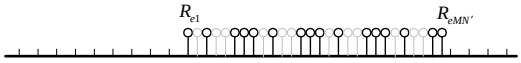

(b) Equivalent transmit and receive collocated sparse linear array

Figure 1. MIMO sparse linear array and its equivalent array

When sparse, in order not to affect the azimuth resolution, it is necessary to ensure that the total aperture length of the equivalent array remains unchanged, that is, the position of the receiving array elements at both ends of the linear array remains unchanged, Among the N receiving arrays, N' are randomly selected and reserved, and MN' virtual receiving arrays are obtained by PCA. Define the sparsity as $\Gamma = (1 - N'/N) \times 100\%$.

Sparse linear array adopts the structure shown in Figure 1, which is established at the position parallel to the x-axis $(y = y_b)$. The position coordinate of the scattering point target is set as $Q(x_q, y_q)$, the reference center of the target is set at the $A(x_a, y_a)$ which is the origin of coordinates , and the position coordinate of the uniform transmitting array of the spacing Nd is expressed as $[x_{t1}, x_{t2}, \cdots, x_{tm}]$. without sparse, the receiving array is a uniform array of the spacing d, the sparse coordinate is $[\tilde{x}_{r1}, \tilde{x}_{r2}, \cdots, \tilde{x}_{rN'}]$, and the equivalent transmitting and receiving virtual array is approximated by the PCA. The position coordinate is $[x_{e1}, x_{e2}, \cdots, x_{eMN'}]$ and the interval is $d/2$.

The distance from the scattering point Q of the target to the m-th transmitting array element is represented by $T_m Q$, the distance from the point Q to the corresponding n'-th receiving array element is represented by $QR_{n'}$, the distance from the target to the m-th transmitting array element and the n'-th receiving array element passing through the PCA equivalent virtual array element is $E_i Q$, and the distance from the target reference center A to the equivalent array element is $E_i A$. Under the far-field condition, the sum of distance between $T_m Q$ and $QR_{n'}$ is:

$$\begin{aligned} T_m Q + QR_{n'} &= \sqrt{(x_q - x_{tm})^2 + (y_b - y_q)^2} + \sqrt{(x_q - \tilde{x}_{rn'})^2 + (y_b - y_q)^2} \\ &\approx y_q - y_b + \frac{(x_{tm} - x_q)^2}{2(y_q - y_b)} + y_q - y_b + \frac{(x_q - \tilde{x}_{rn'})^2}{2(y_q - y_b)} \\ &= 2\sqrt{(y_q - y_b)^2 + (x_q - x_{ei})^2} + \frac{(x_{tm} - \tilde{x}_{rn'})^2}{4(y_q - y_b)} \end{aligned} \tag{1}$$

Where, $x_{ei} = \dfrac{x_{tm} + \tilde{x}_{rn'}}{2}$ It represents the equivalent virtual array element position of T_m and $R_{n'}$.

If $\sqrt{(y_q - y_b)^2 + (x_q - x_{ei})^2}$ is recorded as $E_i Q$ and $(x_{tm} - \tilde{x}_{rn'})^2 / 4(y_q - y_b)$ as $\Delta E_i Q$, then formula (1) can be simplified as:

$$T_m Q + QR_{n'} = 2E_i Q + \Delta E_i Q \tag{2}$$

$E_i Q$ represents the distance from Q to the equivalent array, and $\Delta E_i Q$ represents the error phase generated by the approximate process of the phase center, which needs to be compensated in the subsequent processing, otherwise, the phase defocusing will affect the imaging quality.

The transmitted signal still adopts phase coded signal. Since M transmitted signals irradiate the scattering point Q of the target, the echo signal of the n'th receiving array element is a mixture of M signals. After removing the carrier frequency of the signal, it can be expressed as follows:

$$\begin{aligned} s_{n'}(t) = \sigma_q \sum_{m=1}^{M} \exp\left\{-j2\pi\left(T_m Q + QR_{n'}\right)/\lambda + j\phi_m\left[t-\left(T_m Q + QR_{n'}\right)/c\right]\right\} \\ \left(n = 1, 2, \cdots, N'\right) \end{aligned} \tag{3}$$

Where, σ_q is the scattering coefficient of scattering point Q, c is the speed of light, and λ is the carrier wavelength

The waveform of the mixed echo signal is separated. After separation, the signal echo of the n'th receiving array element irradiated by the m-th transmitting array element is as follows:

$$s_{n'}(t,m) = \sigma_q p[t - \frac{(T_m Q + QR_{n'})}{c}]\exp[-j2\pi\frac{(T_m Q + QR_{n'})}{\lambda}] \tag{4}$$

Where, $p(t)$ is the correlation function of phase coded signal, equation (5) can be fourier transformed to:

$$s_{n'}(f,m) = \sigma_q R(f)\exp[-j2\pi(T_m Q + QR_{n'})(\frac{f}{c}+\frac{1}{\lambda})] \tag{5}$$

Where a is the frequency domain representation of B, take equation (4.2) into equation (4.5) to get:

$$s_{n'}(f,m) = \sigma_q R(f)\exp[-j2\pi(E_i Q + \Delta E_i Q)(\frac{f}{c}+\frac{1}{\lambda})] \tag{6}$$

Multiply equation (6) by $\exp(j2\pi\Delta E_i Q(\frac{f}{c}+\frac{1}{\lambda}))$ for distance compensation, and then perform inverse Fourier transform to obtain the signal received by the equivalent transceiver array:

$$s_{n'}(t, x_{ei}) = \sigma_q p\left(t - \frac{2y_q}{c}\right)\exp\left(-j4\pi\frac{E_i Q}{\lambda}\right) \tag{7}$$

Where, $E_i Q \approx y_q + (-2x_q x_{ei} + x_{ei}^2)/2y_q$.

The azimuth compression can be realized by multiplying $s_{n'}(t, x_{ei})$ by $\exp(j2\pi\Delta E_i Q(\frac{f}{c}+\frac{1}{\lambda}))$. the compressed signal is:

$$\tilde{s}_{n'}(t, x_{ei}) = \sigma_q p(t - \frac{2y_q}{c})\exp(-j4\pi\frac{y_q}{\lambda})\exp(-j4\pi\frac{x_q}{y_q}x_{ei}) \tag{8}$$

The echo of all receiving channels is represented by $\boldsymbol{Y} = \left\{\tilde{s}_{n'}(t, x_{e1})^H, \tilde{s}_{n'}(t, x_{e2})^H, \cdots, \tilde{s}_{n'}(t, x_{eMN'})^H\right\}$. obviously, the dimension of data matrix $\boldsymbol{Y}$ is $L \times MN'$, where L is the number of range vectorization elements and MN' is the number of PCA equivalent virtual elements. Because the dimension of the echo data matrix $\tilde{\boldsymbol{Y}}$ of the uniform linear array without sparse processing is $L \times MN$, that is, the number of the range vectorization elements is L, and the number of the equivalent virtual elements is MN. Therefore, each distance element data of $\boldsymbol{Y}$ can be regarded as a low dimensional observation of full array data $\tilde{\boldsymbol{Y}}$, and the observation matrix $\boldsymbol{\Phi} = \left\{\phi_{\mu,\nu}\right\}$ is a generalized unit matrix:

$$\phi_{\mu,\nu} = \begin{cases} 1, \nu = \delta_\mu, \mu = 1, \cdots, MN', \delta_\mu \in 1, \cdots, MN \\ 0, \text{else} \end{cases} \tag{9}$$

Where, δ_μ is consistent with the sparse position of the equivalent virtual array element.

Sparse basis $\boldsymbol{\Psi}$ is IDFT transformation matrix:

$$\boldsymbol{\Psi}=\frac{1}{MN}\begin{bmatrix}1 & 1 & \cdots & 1\\ 1 & Z_{MN}^{-1} & \cdots & Z_{MN}^{-(MN-1)}\\ \vdots & \vdots & \ddots & \vdots\\ 1 & Z_{MN}^{-(MN-1)} & \cdots & Z_{MN}^{-(MN-1)^2}\end{bmatrix} \tag{10}$$

Where, $Z_{MN}=\exp\left(-j\frac{2\pi}{MN}\right)$, Because the receiving elements of sparse array are random missing, $\boldsymbol{\Psi}$ and $\boldsymbol{\Phi}$ satisfy rip criterion. Assuming that the scattering point distribution of the target in the l -th(l=1,$\cdots$,L) distance element is recorded as $\boldsymbol{X}_l$ as $\boldsymbol{a}$, and the l row of matrix $\boldsymbol{Y}$ is recorded as $\boldsymbol{y}$, then according to the sparse recovery theory, $\boldsymbol{a}$ can be obtained by solving the following formula:

$$\begin{aligned}&\min \|\boldsymbol{a}\|_0\\ &s.t.\ \boldsymbol{y}=\boldsymbol{\Theta a}\end{aligned} \tag{11}$$

Where, $\boldsymbol{\Theta}=\boldsymbol{\Phi\Psi}$ By solving a with equation (11), we can get the scattering point distribution of all distance elements of the target, that is, the two-dimensional image of the target

3. Sparse MIMO linear array imaging based on Localized Low-rank Promoting algorithm

3.1. Local rank minimization for sparse imaging

In the MIMO sparse array radar imaging scene, transform equation (11) into the following signal model

$$\boldsymbol{y}=\boldsymbol{\Theta a}+\boldsymbol{w} \tag{12}$$

Where, $\boldsymbol{y}\in R^{MN'\times 1}$ is the sparse array observation signal, $\boldsymbol{a}\in R^{MN\times 1}$ is the target image to be reconstructed, $\boldsymbol{\Theta}\in R^{MN'\times MN}\left(MN'<MN\right)$ is the perception matrix, and $\boldsymbol{w}\in R^{MN\times 1}$ is the error and noise. There is block structure coefficient in MIMO echo signal, which contains block related information, but the location of block structure is unknown. In order to realize the reconstruction of signal $\boldsymbol{a}$ in equation (12), the matrix $\boldsymbol{A}\triangleq\begin{bmatrix}0,\boldsymbol{a}\\ \boldsymbol{a},0\end{bmatrix}\in R^{(N+1)\times 2}$ is constructed. Suppose $\boldsymbol{X}_i$ represents the 2×2 submatrix composed of line i and line $i+1$ of $\boldsymbol{X}$, as follows:

$$\boldsymbol{A}_i\triangleq\begin{bmatrix}a_{i-1} & a_i\\ a_i & a_{i+1}\end{bmatrix} \tag{13}$$

Where a_i represents the i -th element of $\boldsymbol{a}$, where a_{i-1}, a_i and a_{i+1} are all zero, then the rank of $\boldsymbol{A}_i$ is 0. When a_{i-1}, a_i and a_{i+1} are not zero and are locally smooth, the rank of $\boldsymbol{A}_i$ is approximately 1. Therefore, the non-zero element solution of vector $\boldsymbol{a}$ is transformed into the rank minimum solution of matrix $\{\boldsymbol{A}_i\}$, that is:

$$\begin{aligned}&\min_{\boldsymbol{x}} \quad \sum_{i=1}^{N}\operatorname{rank}\left(\boldsymbol{A}_i\right)\\ &\text{s.t.} \quad \|\boldsymbol{y}-\boldsymbol{\Theta a}\|_2\le\varepsilon\end{aligned} \tag{14}$$

ε is the error tolerance parameter related to noise statistics.

3.2. Local rank minimization for sparse imaging

Matrix rank minimization problem is a NP hard problem. In order to avoid this problem, using $\log\left|\boldsymbol{A}_i\boldsymbol{A}_i^H\right|=2\sum_i\log\nu_j$, where ν_j represents the j -th singular value of $\boldsymbol{A}_i$, the solution of matrix rank is transformed into the relatively easy solution of logarithmic determinant function [7]

$$\begin{aligned} \min_{\boldsymbol{x}} \quad & \sum_{i=1}^{N} \log\left|\boldsymbol{A}_i \boldsymbol{A}_i^H + \boldsymbol{E}\right| \\ \text{s.t.} \quad & \left\|\boldsymbol{y} - \boldsymbol{\Theta a}\right\|_2 \le \varepsilon \end{aligned} \tag{15}$$

Where $\boldsymbol{E}$ is a positive definite matrix:

$$\boldsymbol{E} \triangleq \delta \begin{bmatrix} 1 & \tau \\ \tau & 1 \end{bmatrix} \tag{16}$$

In order to avoid the algorithm falling into the local minimum because δ is constant, the parameter δ is set as decreasing sequence, that is, $\delta^{(t+1)} = \delta^{(t)}/10$, $(\cdot)^{(t)}$ represents the result of the t-th iteration variable, vector or matrix of a times. Parameter τ is selected as follows:

$$\tau = H_{1,2}/H_{1,1} \tag{17}$$

Where, $\boldsymbol{H} \triangleq \boldsymbol{A}^H \boldsymbol{A}$. Usually, $-1 < \tau < 1$. The formula (15) is unconstrained, i.e:

$$\min_{a} L(\boldsymbol{a}) = \sum_{i=1}^{N} \log\left|\boldsymbol{A}_i \boldsymbol{A}_i^{\mathrm{T}} + \boldsymbol{E}\right| + \gamma \left\|\boldsymbol{y} - \boldsymbol{A a}\right\|_2^2 \tag{18}$$

Where, γ is the trade-off parameter, which is used to control the last two weights.

The upper bound of the objective function is minimized by means of the MM algorithm [8]. So equation (18) satisfies the following inequality

$$\log\left|\boldsymbol{A}_i \boldsymbol{A}_i^H + \boldsymbol{E}\right| \le \frac{1}{2}\mathrm{Tr}\left(\left(\boldsymbol{A}_i \boldsymbol{A}_i^H + \boldsymbol{E}\right)\Phi_i^{(t)}\right) + \log\left|\left(\boldsymbol{\Phi}_i^{(t)}\right)^{-1}\right| - 1 \tag{19}$$

Where, $\boldsymbol{\Phi}_i^{(t)} \triangleq \left(\boldsymbol{A}_i^{(t)}\left(\boldsymbol{A}_i^{(t)}\right)^H + \boldsymbol{E}\right)^{-1}$, When $\boldsymbol{A}_i^{(t)} = \boldsymbol{A}_i$, the above equation holds. Therefore,

$$\sum_{i=1}^{N} \log\left|\boldsymbol{A}_i \boldsymbol{A}_i^H + \boldsymbol{E}\right| \le f\left(\boldsymbol{a} \mid \boldsymbol{a}^{(t)}\right) \tag{20}$$

A is called the upper bound function of the logarithm determinant function in control equation (20). when:

$$\boldsymbol{\Phi}_i^{(t)} \triangleq \begin{bmatrix} a^i & b^i \\ c^i & d^i \end{bmatrix} \tag{21}$$

Then formula $f\left(\boldsymbol{a} \mid \boldsymbol{a}^{(t)}\right)$ can be further expressed as:

$$f\left(\boldsymbol{a} \mid \boldsymbol{a}^{(t)}\right) = \boldsymbol{a}^H \boldsymbol{W a} + \sum_{i=1}^{N}\left(\log\left|\boldsymbol{\Phi}_i^{(t)}\right|\right) - N \tag{22}$$

Where, $\boldsymbol{W} \in R^{MN \times MN}$ is a diagonal matrix, and there are nonzero elements on the main diagonal and the upper and lower diagonal of the main diagonal. The positions and shapes of these non-zero elements are similar to $\boldsymbol{W}_{i,i} = \frac{1}{2}(a^i + d^i + d^{i-1} + a^{i+1})$, $\boldsymbol{W}_{i+1,i} = \frac{1}{2}(c^i + c^{i+1})$, $\boldsymbol{W}_{i,i+1} = \frac{1}{2}(b^i + b^{i+1})$, where $d^0 = a^{N+1} = 0$.

Construct the following alternative functions:

$$Q\left(\boldsymbol{a} \mid \boldsymbol{a}^{(t)}\right) = \boldsymbol{a}^H \boldsymbol{W a} + \sum_{i=1}^{N}\left(\log\left|\boldsymbol{\Phi}_i^{(t)}\right|\right) + \gamma \left\|\boldsymbol{y} - \boldsymbol{A a}\right\|_2 - N \tag{23}$$

The optimization problem of equation (18) is transformed into that of iterative minimization (23). The optimal solution can be expressed as follows:

$$\boldsymbol{a} = \left(\boldsymbol{\Theta}^H \boldsymbol{\Theta} + \gamma^{-1} \boldsymbol{\Theta}\right)^{-1} \boldsymbol{\Theta}^H \boldsymbol{y} \tag{24}$$

Therefore, when the optimization problem of iterative minimization (23) is solved, the function is non incremental in each iteration, and finally the MIMO target image reconstructed by LLP algorithm is obtained.

3.3. LLP based sparse MIMO linear array imaging algorithm flow

Input: sparse array signal $\boldsymbol{y}$, sensing matrix $\boldsymbol{\Theta}$, parameters γ and τ, minimum number of iterations T;

Iteration:

1): initialization signal $\boldsymbol{a}^{(0)}=\boldsymbol{\Theta}^{+}\boldsymbol{y}$, the initial setting of the number of iterations is $t=0$;

2) when the solution result is not convergent and $t\le T$, the following iteration 3) to 6) is carried out;

3): calculate $\boldsymbol{\Phi}_i^{(t)}$ and get $\boldsymbol{W}$;

4): a new estimated signal is obtained by equation (24), which is recorded as $\boldsymbol{a}^{(t+1)}$;

5): if the signal satisfies $\left\|\boldsymbol{a}^{(t+1)}-\boldsymbol{a}^{(t)}\right\|_2 \le \sqrt{\delta^{(t)}}/10$, then $\delta^{(t+1)}=\delta^{(t)}/10$;

6): $t=t+1$;

7): when the convergence condition is satisfied, the iteration is stopped and the reconstruction result AA is obtained.

Output: reconstruct the MIMO image data $\boldsymbol{a}$.

4. simulation experiment

4.1 Simulation experiment 1: LLP algorithm reconstruction performance analysis

Set the simulation block sparse signal to test the performance of the algorithm. Consider a block sparse signal $\boldsymbol{x}$, dimension 200, the length of non-zero segmentation block is 4, there are 50 blocks in total, and define the sparsity as K (the number of blocks). The non-zero block position is randomly distributed, and the data in the block follows the standard Gaussian normal distribution. The reconstruction effect is measured by the accurate reconstruction probability, which is defined as $\max_i \left\|\boldsymbol{x}-\hat{\boldsymbol{x}}\right\|_\infty \le 10^{-3}$. Figure 2 shows the results of 200 Monte Carlo simulation experiments of LLP algorithm under different sparsity. With the increase of K, the reconstruction probability of LLP is higher than that of SBL.

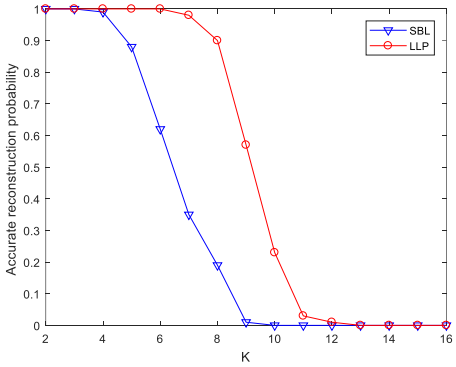

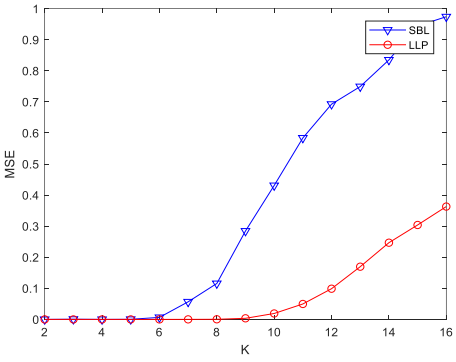

Figure 2. reconstruction probability curve with K Figure 3. curve of MSE with K

Further, the MSE of the reconstructed signal is used for the reconstruction performance of the algorithm under different sparsity. When K changes from 2 to 16, 200 Monte Carlo simulation experiments are conducted, and the relationship curve between MSE and LLP algorithm is shown in Figure 3. It can be seen that the larger the K is, the larger the MSE is; when K is greater than 6, with the increase, the MSE of LLP algorithm is better than that of SBL algorithm, and the greater the K is, the more obvious the advantage is. Simulation results show that the reconstruction accuracy of LLP algorithm is better than that of SBL algorithm.

In order to test the reconstruction performance of LLP algorithm for block sparse signal under different signal-to-noise ratios, make it 10, and the signal-to-noise ratio changes from 2dB to 20dB

with 1dB interval, and carry out 100 Monte Carlo tests. The MSE curve of LLP algorithm and SBL algorithm changes with the signal-to-noise ratio is shown in Figure 4:

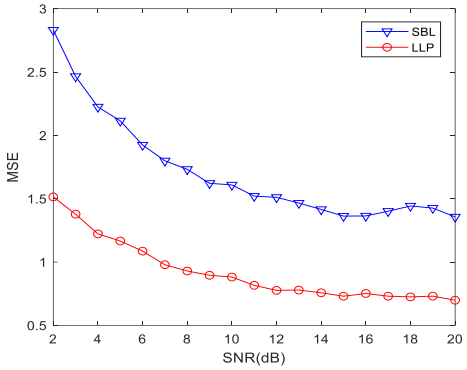

Figure 4. change curve of MSE with SNR

It can be seen from the above figure that with the increase of signal-to-noise ratio, the performance of LLP algorithm and SBL algorithm has been improved, but LLP algorithm always has better reconstruction accuracy, and its reconstruction probability error curve has been under the SBL algorithm, so LLP algorithm has better signal recovery performance for block sparse structure than SBL algorithm.

4.2 Simulation experiment 2: LLP algorithm sparse MIMO linear array imaging experiment

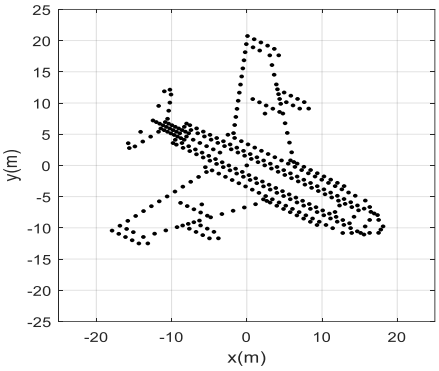

Figure 5. scatter point model

Set the MIMO sparse linear array radar imaging scene, and the scattering point model of the imaging target is shown in Figure 5. The linear array of 4 transmitters and 20 receivers in Figure 1 is established, with the receiving array element spacing of 18m and array sparsity set as $\Gamma = 50\%$. The imaging results of direct IFFT, SBL algorithm and LLP algorithm are shown in Figure 4.6

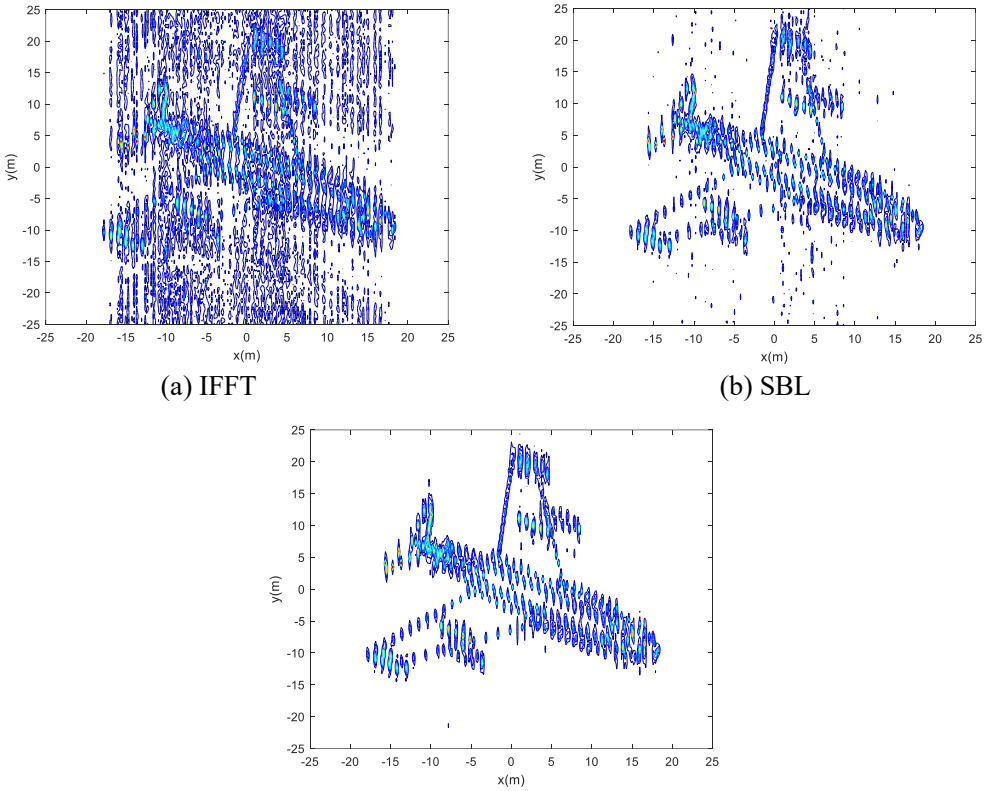

(a) IFFT (b) SBL

(c) LLP

Figure 6. imaging effect of different algorithms

It can be seen from Figure 6 (a) that the sparse array is FFT directly, and the image appears serious defocusing and blurring; Figure 6 (b) the imaging effect is improved compared with Figure 6 (a), and the sparse reconstruction algorithm based on SBL can improve the imaging quality of sparse array, but there are many false points; Figure 6 (c) the imaging effect is further improved compared with SBL, which shows that LLP algorithm utilizes the sparse target block Sparse characteristics improve the imaging quality. MSE of several algorithms is shown in table 1. It can be seen that LLP algorithm has the best imaging effect. It shows that the block sparse reconstruction algorithm takes advantage of the block sparse feature of radar target and can further improve the imaging effect of sparse array.

Table 1 MSE of several algorithms

	IFFT	SBL	LLP
MSE	0.5968	0.3959	0.2293

Further, the array sparsity Γ is increased from 20% to 70% at 10% interval. Repeat 100 Monte Carlo experiments, and the mean square error of sparse linear array imaging obtained by different algorithms is shown in Figure 7. As shown in Figure 7, with the increase of array sparsity, the effectiveness of the three algorithms is poor, but the sparse linear array imaging effect based on LLP algorithm is the best, because LLP algorithm can take advantage of the block sparsity of the target image, which has better imaging effect than the traditional sparse reconstruction algorithm.

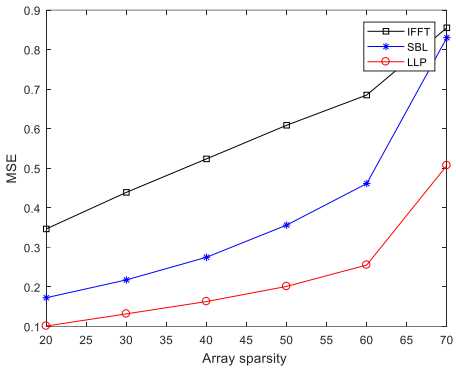

Figure 7. change curve of MSE with sparsity

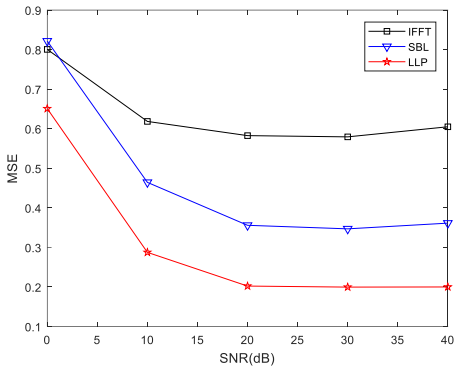

Figure 8. change curve of MSE with SNR

When the array sparsity is fixed to 50%, and the SNR changes from 0dB to 40dB at 10dB intervals, repeat 100 Monte Carlo experiments, and the results are shown in Figure 4.8. It can be seen from figure 8 that the standard deviation of several imaging methods increases with the decrease of signal-to-noise ratio, and the standard deviation of LLP is always lower than that of other methods. It shows that the phase algorithm has better adaptability under different noise conditions

5. conclution

In view of the block sparsity of radar target echo signal, LLP algorithm is used for imaging. The target echo to be reconstructed is transformed into the minimization problem of multiple 2×2 dimension matrix ranks, and the block sparse signal is reconstructed by using a determinant function which can promote the block sparse and local smooth solution. In the process of solving, the optimal solution is obtained by maximizing the minimum method and iteratively minimizing the upper bound of determinant function. The simulation results show that the LLP algorithm has the advantages of different array sparsity and SNR conditions.

References

[1] Wang H., Su Y, Huang C. Research on MIMO radar imaging based on antenna array [J]. Signal Processing, 2009 (8): 1203-1208.
[2] Chen G. Research on sparse array MIMO radar imaging technology [D]. Nanjing University of technology, 2014
[3] Liu H, Jiu B, Liu H, et al. Superresolution ISAR imaging based on sparse Bayesian learning[J]. IEEE Transactions on Geoscience and Remote Sensing, 2013, 52(8): 5005-5013.
[4] Tomei, S., Bacci, A., Giusti, E., et al.: 'Compressive sensing based inverse synthetic radar imaging from incomplete data', IET Radar Sonar Navig.2016, 10, (2), pp. 386–397
[5] Gu F, Chi L, Zhang Q, et al. Single snapshot imaging method in multiple-input multiple-output radar with sparse antenna array[J]. IET Radar, Sonar & Navigation, 2013, 7(5): 535-543.
[6] Wang L., L. Zhao, G. Bi, C. Wan, and L.Yang. Enhanced ISAR imaging by exploiting the continuity of the target scene[J].IEEE Transactions Geoscience and Remote Sensing,2014,52(9):5736-5750
[7] Yang L, Fang J, Li H, et al. Localized low-rank promoting for recovery of block-sparse signals with Intrablock correlation[J]. IEEE Signal Processing Letters, 2016, 23(10): 1399-1403.
[8] Lange H K . A tutorial on MM algorithms [J]. The American Statistician, 2004, 58(1):30-37.